

# Massive Dirac-Pauli physics in lead-halide perovskites

Abhishek Shiva Kumar<sup>1</sup>, Mikhail Maslov<sup>1</sup>, Mikhail Leshko<sup>1</sup>,

Artem G. Volosniev<sup>1,2,\*</sup> and Zhanybek Alpichshev<sup>1†</sup>

<sup>1</sup>*Institute of Science and Technology Austria (ISTA),*

*Am Campus 1, 3400 Klosterneuburg, Austria and*

<sup>2</sup>*Department of Physics and Astronomy, Aarhus University,*

*Ny Munkegade 120, DK-8000 Aarhus C, Denmark*

(Dated: July 8, 2024)

In standard quantum electrodynamics (QED), the so-called non-minimal (Pauli) coupling is suppressed for elementary particles and has no physical implications. Here, we show that the Pauli term naturally appears in a known family of Dirac materials – the lead-halide perovskites, suggesting a novel playground for the study of analogue QED effects. We outline measurable manifestations of the Pauli term in the phenomena pertaining to (i) the Klein paradox and (ii) relativistic corrections to bound states. In particular, we demonstrate that the binding energy of an electron in the vicinity of a positively charged defect is noticeably decreased due to the polarizability of lead ions and the appearance of a Darwin-like term. Our study adds to understanding of quantum phenomena in lead-halide perovskites, and paves the way for tabletop simulations of analogue Dirac-Pauli equations.

## I. INTRODUCTION

The band structure of certain condensed matter systems (Dirac materials) resembles the energy spectrum of the single-body relativistic problem [1]. Arguably, the best known system of this type is graphene whose massless Dirac-like band structure leads to a number of remarkable physical phenomena that were previously discussed mainly in the context of relativistic high-energy physics [2]. Topological insulators and Weyl semimetals are among the other celebrated examples [3–5]. These materials have become the tabletop experimental platforms for visualizing the extreme relativistic phenomena that obey conventional particle theories, such as QED. The natural question that may arise in this context is whether the analog Dirac materials can help to study conceivable high-energy effects that fall beyond the Standard Model of elementary particles.

The coupling of Dirac materials to electromagnetic fields is typically given via a minimal substitution:  $p^\nu \rightarrow p^\nu - qA^\nu$ , where  $p^\nu$  and  $A^\nu = (\phi, \mathbf{A})$  are the usual four-momentum and electromagnetic four-potential, respectively [6]. However, Lorentz and gauge invariance allow in general for additional ‘non-minimal’ couplings to electromagnetic fields (see, e.g., Ref. [7]). The first such extension of the Dirac equation was suggested by Pauli [8] who introduced what is now known as the Dirac-Pauli equation [9]

$$\left( \gamma^\nu (p_\nu - qA_\nu) - \frac{i\mu'}{4} [\gamma_\mu, \gamma_\nu] F^{\mu\nu} - m \right) \psi = 0. \quad (1)$$

Here,  $\gamma^\nu$  are the Dirac matrices,  $F^{\mu\nu}$  is the electromagnetic field tensor,  $m$  is the rest mass of the Dirac particle

and  $\mu'$  is its anomalous moment. The experimental data on magnetic moments of elementary particles suggest that  $\mu'$  is negligibly small [10]. It can even be assumed that  $\mu' = 0$  at the current state of our understanding of quantum electrodynamics [11]. Therefore, the Pauli term is typically neglected with rare exceptions of effective quantum field theories that aim to include polarizabilities of composite particles such as neutrons and protons [12–14] in a phenomenological way.

Here, we show that the Pauli term naturally appears in the low-energy description of lead-halide perovskites (LHPs), making it (to the best of our knowledge) the first known Dirac-Pauli semiconductor. Lead-halide perovskites is a family of advanced energy materials [15] with exceptional optoelectronic properties [16, 17]. Charge carriers in LHPs can be described by the massive Dirac equation [18, 19] with a peculiarity that their coupling to electromagnetic fields requires an explicit inclusion of the high polarizability of  $\text{Pb}^{2+}$  ions [20, 21]. Here, we first illustrate that this non-standard matter-field interaction is actually the Pauli coupling with the (effective) atomic dipole polarizability in place of the anomalous moment,  $\mu'$ . Further, to facilitate future theoretical and experimental studies, we outline a few effects that the Dirac-Pauli physics can have on the properties of LHPs. In particular, we consider scattering off a step potential and binding of charge carriers to local defects, such as vacancies and interstitials.

## II. RESULTS

**Pauli coupling in LHPs.** The Hilbert space for the low-energy description of LHPs is determined by the hybridization of orbitals of lead and halide atoms [22]. In the vicinity of the chemical potential, the states have predominantly  $s$ - (valence band) and  $p$ -type (conduction band) characters [18, 19]. Strong spin-orbit cou-

\* artem@phys.au.dk

† alpichshev@ist.ac.at

pling splits the  $p$ -type states. Therefore, both the top of the valence band and the bottom of the conduction band have  $J = 1/2$ , and low-energy optoelectronic properties of LHPs are shaped by four states that can be conveniently written as  $\{|\uparrow\uparrow\rangle, |\downarrow\uparrow\rangle, |\uparrow\downarrow\rangle, |\downarrow\downarrow\rangle\}$ , where

$$\begin{aligned} |\uparrow\uparrow\rangle &= -(|p_z\rangle|\uparrow\rangle + (|p_x\rangle + i|p_y\rangle)|\downarrow\rangle)/\sqrt{3}, \\ |\uparrow\downarrow\rangle &= (|p_z\rangle|\downarrow\rangle - (|p_x\rangle - i|p_y\rangle)|\downarrow\rangle)/\sqrt{3}, \\ |\downarrow\uparrow\rangle &= |s\rangle|\uparrow\rangle, \quad |\downarrow\downarrow\rangle = |s\rangle|\downarrow\rangle. \end{aligned} \quad (2)$$

The right-hand-side of these expressions follows the standard notation [23, 24] for the spin structure of the state  $[|\downarrow\rangle]$  and  $[|\uparrow\rangle]$  and for its spatial component  $[|s\rangle, |p_x\rangle, |p_y\rangle, |p_z\rangle]$ . The Hermitian operators that act in the Hilbert space of Eq. (2) can be readily written as the direct product  $\tau_i \otimes \sigma_j$ , where  $\tau_i$  and  $\sigma_j$  are the Pauli matrices that operate correspondingly in the orbital ( $\{|\uparrow\rangle, |\downarrow\rangle\}$ ) and the quasi-spin ( $\{|\uparrow\rangle, |\downarrow\rangle\}$ ) subspaces defined via the left-hand-side of the equations.

In the absence of external fields, the low-energy spectrum of LHPs is determined by diagonalizing the Hamiltonian ( $\hbar = c = 1$ ) [18]:

$$H = \Delta(\mathbf{k})\tau_3 \otimes \mathbb{I} + 2at \tau_2 \otimes \boldsymbol{\sigma} \cdot \mathbf{k}, \quad (3)$$

where  $\boldsymbol{\sigma}$  is a vector of Pauli matrices, so that  $\boldsymbol{\sigma} \cdot \mathbf{k} = \sum_i \sigma_i k_i$ .  $\Delta(\mathbf{k}) = \frac{1}{2} \left( \Delta + \frac{t_3 a^2 |\mathbf{k}|^2}{2} \right)$ ,  $\mathbf{k}$  is the quasi-momentum counted from the high-symmetry  $R$ -point relevant for low-energy physics of LHPs,  $\Delta$  is the bandgap at the  $R$ -point,  $a$  is the lattice constant,  $t_3$  and  $t$  are further  $\mathbf{k} \cdot \mathbf{p}$  parameters of the Hamiltonian. They can be estimated by fitting to numerical calculations or experimental data. For example, for methylammonium lead bromide (MAPbBr<sub>3</sub>) these parameters are found to be:  $t \simeq 0.6\text{eV}$ ,  $t_3 \simeq 0.9\text{eV}$ ,  $a \simeq 0.586\text{nm}$ ,  $\Delta \simeq 2.3\text{eV}$  [19, 21].

It was recently shown both experimentally and theoretically that in order to account for the full effect of the external electric field  $\mathbf{E}$  on LHPs, one should employ not only the minimal coupling  $\tilde{\mathbf{k}} = \mathbf{k} - q\mathbf{A}$  (where  $q$  is the charge of an electron) in Eq. (3) but also an additional term  $\mu \tau_1 \otimes \boldsymbol{\sigma} \cdot \mathbf{E}$ , dubbed ‘spin-electric’ in Refs. [20, 21] because it couples the quasi-spin degree of freedom to an external electric field. The non-minimal coupling term accounts for the local effects of the electric field on the lattice, in particular, on the highly polarizable Pb<sup>2+</sup>. Therefore, we interpret  $\mu$  as coming from the effective atomic polarizability of lead ions. For MAPbBr<sub>3</sub>, the experiment demonstrates that the magnitude of this effect corresponds to  $\mu \simeq -0.3|q|a$  [21].

A close examination reveals that the operator  $\mu \tau_1 \otimes \boldsymbol{\sigma} \cdot \mathbf{E}$  is nothing else but the electric part of the Pauli term in Eq. (1). Indeed, the Hamiltonian in Eq. (3) amended with the spin-electric term can be written as:

$$H = \Delta(\tilde{\mathbf{k}})\beta + 2at\boldsymbol{\alpha} \cdot \tilde{\mathbf{k}} + i\mu\boldsymbol{\gamma} \cdot \mathbf{E}, \quad (4)$$

where  $\beta = \tau_3 \otimes \mathbb{I}$ ,  $\boldsymbol{\alpha} = \tau_2 \otimes \boldsymbol{\sigma}$ , and  $\boldsymbol{\gamma} = \beta\boldsymbol{\alpha}$ . As the matrices  $\boldsymbol{\gamma}^\nu = \{\beta, \boldsymbol{\gamma}\}$  satisfy the Dirac algebra

$\{\boldsymbol{\gamma}^\mu, \boldsymbol{\gamma}^\nu\} = \text{diag}(2, -2, -2, -2)$ , the first two terms in Eq. (4) lead to the Dirac equation in Eq. (1) with  $\mu' = 0$  and  $t_3 = 0$ . [The ‘standard (Dirac) representation’ of the gamma matrices [9] is obtained by the unitary transformation  $U^\dagger \boldsymbol{\alpha} U$  where  $U = e^{-i\tau_3 \pi/4}$ , which corresponds to a  $\pi/2$ -rotation in the  $\tau$ -subspace.] Note that  $t_3 \neq 0$  is beyond the Dirac equation, as is common for gapped Dirac materials [25]. We note that while this term does not break the algebraic structure of the Dirac equation its presence leads to measurable consequences, e.g., in the determination of the energy of a bound state in an impurity potential (see below).

Finally, in the absence of magnetic fields  $[\boldsymbol{\gamma}^\mu, \boldsymbol{\gamma}^\nu]F^{\mu\nu} = 4\boldsymbol{\gamma} \cdot \mathbf{E}$ , establishing equivalence between Eqs. (1) and (4) with  $\mu' = \mu$ . Note that the magnetic part of the Pauli term  $[\boldsymbol{\gamma}^\mu, \boldsymbol{\gamma}^\nu]F^{\mu\nu}$  leads to an anomalous  $\tau_3 \otimes \boldsymbol{\sigma} \cdot \mathbf{B}$  coupling, which also enters the low-energy description of LHPs placed in the magnetic field  $\mathbf{B}$  [20, 21]. However, the precise magnitude of this magnetic term in MAPbBr<sub>3</sub> is currently undetermined, and therefore, we leave the corresponding investigation to future studies.

In what follows, we illustrate the physical implications of the Pauli term for LHPs. To this end, we solve the stationary Dirac-Pauli equation

$$H\Psi = \mathcal{E}\Psi, \quad (5)$$

where  $\Psi$  is the 4-component Dirac spinor,  $\Psi^T = (\psi_{\uparrow\uparrow}, \psi_{\uparrow\downarrow}, \psi_{\downarrow\uparrow}, \psi_{\downarrow\downarrow})$ , and  $\mathcal{E}$  is the energy. [Here, the first (last) two elements of the spinor are typically referred to as electron (hole) components.] Specifically, we solve Eq. (5) with the Dirac-Pauli Hamiltonian for two standard physical problems: scattering of free charge carriers off a potential step (Klein paradox; see Fig. 1(a)) and determination of the energy of bound states in the vicinity of an attractive potential.

**Klein problem in LHPs.** Klein paradox refers to a counter-intuitive behavior of scattering amplitudes off a step potential whose height is larger than twice the particle’s rest mass. In the first quantization picture, the paradox manifests itself in the seemingly unphysical values for the reflection and transmission coefficients. In particular, the Klein’s solution suggests that the transmitted current does not vanish even when the height of the barrier approaches infinity [26, 27] (for more details see Refs. [28–30]).

Direct experimental observation of this physics in quantum electrodynamics would require access to extremely high electric fields not available in modern laboratories [31]. This motivates searches for tabletop setups that would realize Dirac’s equation, such as gapless Dirac materials [32, 33] or photonic superlattices [34]. The most direct analogy to the Klein paradox in its original formulation however requires working with gapped Dirac semiconductors such as LHPs. The corresponding bandgap  $\Delta$  then would play the role of a pair-creation energy  $2mc^2$  in QED, where  $m$  is the mass of the particle that is being created. As the gap  $\Delta$  can be about six orders of magnitude lower than  $2mc^2$  the corresponding

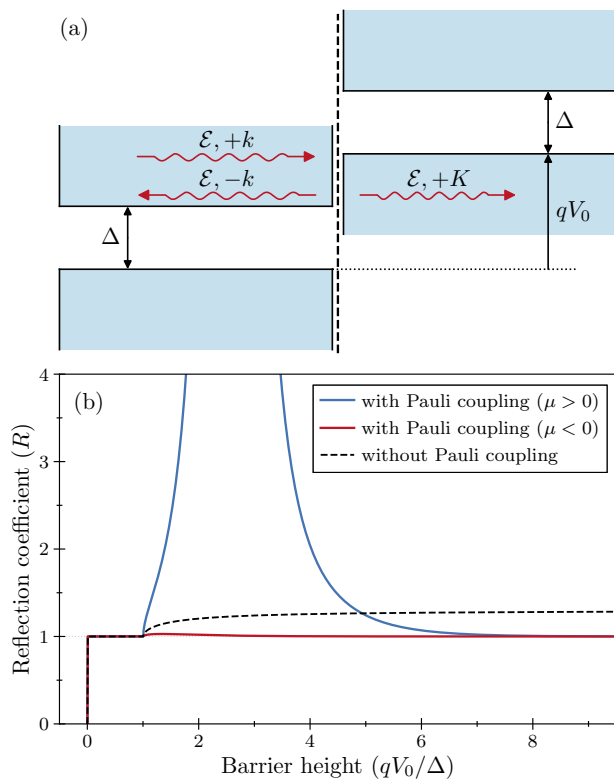


FIG. 1. (a) Schematic of the Klein problem: Electrons of energy  $\mathcal{E}$  and momentum  $k$  are incident on a potential barrier of height  $V_0$ . If the value of  $V_0$  is larger than the energy gap,  $\Delta$ , between the conduction and valence bands, then Klein paradox occurs – particles with momentum  $K$  appear in the high potential region. (b) Reflection coefficient as a function of the (dimensionless) barrier height with and without Pauli coupling assuming that  $\mathcal{E} = 0.01$  eV. The other parameters correspond to MAPbBr<sub>3</sub> with  $\mu < 0$ . For  $\mu > 0$ , only the sign of  $\mu$  is changed in comparison to the case with  $\mu < 0$ .

effects in Dirac semiconductors are much more accessible as compared to QED. Nevertheless, it should be noted that the very existence of an energy gap of a few eV may already result in a considerable experimental obstacle for the observation of Klein paradox in LHPs. Still, we find it fitting to start the discussion of the effect of the Pauli term by considering the corresponding solution of the Dirac equation.

For simplicity, we assume that  $t_3 = 0$  here. Similar to the original formulation of the problem by Klein, we consider the one-dimensional potential

$$\phi(x) = V_0 \Theta(x), \quad (6)$$

where  $\Theta(x)$  is the Heaviside step function, and  $V_0$  is the strength of the potential. For  $\mu \neq 0$ , the associated electric field  $E_x = -\partial\phi/\partial x = -V_0\delta(x)$  enters the Dirac equation via the Pauli term. This leads to a term with a  $\delta$ -function in Eq. (4), giving rise to a discontinuity in the spinor components at  $x = 0$ , which can be treated as a specific boundary condition.

We solve the Dirac-Pauli equation for each spinor component and arrive at the following expressions for the reflection and transmission coefficients (see Suppl. Note 1):

$$R = \left| \frac{r-1}{r+1} \right|^2, \quad T = \frac{\text{Im}\Lambda}{\lambda} \frac{4|r|^2}{|r+1|^2} e^{\frac{\mu V_0}{at}}, \quad (7)$$

where  $\lambda = 4iatk/(\Delta + 2\mathcal{E})$  and  $\Lambda = 4iatK/(\Delta + 2\mathcal{E} - 2qV_0)$ ,  $r = \lambda e^{-\frac{\mu V_0}{at}}/\Lambda$  and  $k$  and  $K$  are the momenta of the charge carrier for  $x < 0$  and  $x > 0$ . For  $\mu \rightarrow 0$ , these expressions turn into the original Klein solution [30]. Non-vanishing values of  $\mu$  lead an exponential dependence on  $V_0$  in Eq. (7). Depending on the sign of  $\mu$ , the exponent  $e^{-\frac{\mu V_0}{at}}$  that appears in the parameter  $r$  is either increasing or decreasing, leaving marked imprints on the transmission and reflection coefficients.

When  $\mu < 0$  as in LHPs, the Klein paradox is modified in comparison to the case when there is no Pauli coupling. Curiously, the introduction of the Pauli term suppresses the anomalous ( $R > 1$ ) Klein reflectivity in the asymptotic limit of large barrier heights,  $qV_0 \rightarrow \infty$ . Figure 1(b) illustrates this for the parameters of MAPbBr<sub>3</sub>. The behavior of the reflection coefficient for  $\mu > 0$  is even more intriguing as it features a resonance-like divergent behavior, which can be interpreted as a resonant enhancement of particle-antiparticle creation within the potential barrier. This might be indicative of a novel vacuum breakdown channel that has previously been overlooked (see Suppl. Note 2 for additional details). We conclude that for the either sign of  $\mu$ , Pauli coupling strongly affects Klein's physics.

#### Bound states near static impurities in LHPs.

In this subsection, we investigate how the bound states of an electron in the vicinity of a spherically symmetric local impurity potential,  $\phi$ , are modified by the Pauli term. To this end, we focus on the effective behavior of electrons by integrating out the hole degrees of freedom following the procedure of Ref. [35] (see Suppl. Note 3), which resembles Foldy-Wouthuysen transformation in QED [36].

By doing so, we frame the problem in the form of the Schrödinger equation for electrons

$$\left( -\frac{\nabla^2}{2m_e^*} + q\phi(r) - \frac{q^2\phi(r)^2}{\Delta} + H_P \right) \psi(r) = \epsilon\psi(r), \quad (8)$$

where  $\psi^T = (\psi_{\uparrow\uparrow}, \psi_{\uparrow\downarrow})$  is the electronic wavefunction;  $\epsilon = \mathcal{E} - \Delta/2$  is the corresponding energy;  $m_e^* = (8a^2t^2/\Delta + t_3a^2/2)^{-1}$  is the effective mass, note that the parameter  $t_3$  enters only in the effective mass, otherwise its presence does not affect our results;  $q\phi(r) - \frac{q^2\phi(r)^2}{\Delta}$  is the potential energy of an electron in the electric field generated by the impurity;  $H_P$  is the sum of terms arising from Pauli coupling:

$$H_P = \frac{|\mu\mathbf{E}(\mathbf{r})|^2}{\Delta} - \frac{2at\mu}{\Delta} \nabla \cdot \mathbf{E}(\mathbf{r}) - \frac{8at\mu}{\Delta} \frac{|\mathbf{E}(\mathbf{r})|}{r} \mathbf{S} \cdot \mathbf{L}. \quad (9)$$

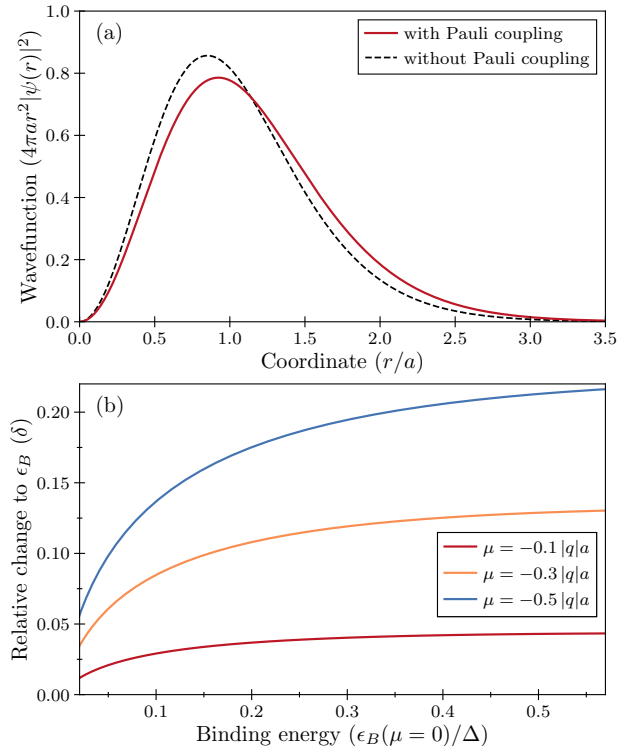


FIG. 2. (a) Ground state wavefunction with and without the Pauli term for  $\frac{\mu}{aq} = 0.3$ . (b) Relative change in the binding energy due to the Pauli coupling plotted as a function of the binding energy with  $H_P = 0$ . Note that the Pauli coupling leads to a decrease in the binding energy. Different curves are for different values of the effective dipole moment,  $\mu$ ; the curve in the middle is calculated with the parameters of MAPbBr<sub>3</sub>.

The first term in  $H_P$  mimics the effect of polarizability of quasi-electrons. This term is non-vanishing even if  $t = 0$ , implying that this polarizability of electrons inside lead-halide perovskites can be traced back to the atomic polarizability of the underlying lattice ions (primarily Pb<sup>2+</sup>), see also the Discussion section below. The  $\nabla \cdot \mathbf{E}(\mathbf{r})$  term is referred to as the Darwin term; in QED, this term is interpreted as coming from the jitter motion (*Zitterbewegung*) of a relativistic electron on the background of a non-uniform electric field [36]. The last term in  $H_P$  describes the spin-orbit coupling (SOC).

If  $\mu \neq 0$ , SOC appears as  $\sim \mu |\mathbf{E}(\mathbf{r})| \mathbf{S} \cdot \mathbf{L} / (r \sqrt{m_e^* \Delta})$  in the effective Schrödinger equation (8) of the Dirac-Pauli system. Hence, its influence on the states and energies is different when compared to a Dirac system of an electron in a given electric field. For example, in a hydrogen atom SOC has the paradigmatic form  $\sim q |\mathbf{E}(\mathbf{r})| \mathbf{S} \cdot \mathbf{L} / (r m_e \Delta)$  [36]. We see that the above presented terms have identical functional dependence. However, their strengths are different with the ratio  $\mu \sqrt{m_e^* \Delta}$ . A similar conclusion can be reached also for the Darwin-like term.

To illustrate the effect of  $H_P$  on the properties of bound states, we investigate the ground state of an electron interacting with a model Gaussian defect whose charge density is chosen as

$$\rho(r) = \frac{Q}{(a\sqrt{\pi})^3} e^{-\frac{r^2}{a^2}}, \quad (10)$$

where  $Q$  is the charge of the defect. The width of the Gaussian is determined by the lattice constant,  $a$ , to model a single-site defect of a semiconductor. We consider a defect with  $Q > 0$ , which binds electrons. However, the hole-electron symmetry allows us to also easily understand what happens for  $Q < 0$  from our calculations.

The charge density produces a radial electric field given by

$$E(r) = \frac{Q}{4\epsilon\pi^{3/2}ar^2} \left( a\sqrt{\pi} \operatorname{erf}(r/a) - 2re^{-\frac{r^2}{a^2}} \right), \quad (11)$$

where  $\epsilon$  is the (dynamic) dielectric constant of the medium and erf is the standard error function. Once the electric field is known, we solve the Schrödinger equation (30) numerically by diagonalizing the corresponding matrix (see Suppl. Note 3). Specifically, we calculate the ground state energy of the system with and without  $H_P$ , and study the difference introduced by  $H_P$ .

For the ground state  $L = 0$ , hence, the spin-orbit coupling term does not play a role in Eq. (31) and can be ignored. In other words, effects of SOC can only be seen in excited states. A study of the ground state allows us to demonstrate the effect of the first two terms in  $H_P$ : the polarizability and the Darwin terms. Note that in LHPs, the parameter  $\mu$  is negative, which implies that the matrix  $H_P$  is positive-definite, and hence, that the ground state energy is increased by the presence of the Pauli coupling.

We show our findings in Fig. 2. First, we plot the electronic density in Fig. 2(a). We see that the wavefunction becomes spatially broader as the Pauli term repels the electron. This change in the electronic density affects other observables as well, for example the binding energy  $\epsilon_B > 0$  of the electron-defect system. Indeed, Fig. 2(b) confirms that the Pauli term leads to a noticeable reduction of  $\epsilon_B$ . In the figure, we plot the relative decrease in binding energy:

$$\delta = \frac{\epsilon_B(\mu=0) - \epsilon_B(\mu)}{\epsilon_B(\mu=0)}. \quad (12)$$

We conclude that the Pauli coupling in lead-halide perovskite can have a measurable effect on the energies of electrons in the vicinity of defects. This effect scales with the parameter  $\mu$ , which depends on the chemical structure of the material. As we expect that  $\mu$  can be affected by one's choice of the halogen atom, further studies are needed to determine the lead-halide perovskite with the most pronounced effect of Pauli coupling for tabletop simulations of the corresponding physics.

### III. DISCUSSION

It was noted by Foldy that the presence of the Pauli term implies finite polarizability of the particle in question [13]. Indeed, for a Hamiltonian of the form  $H = \beta m + \boldsymbol{\alpha} \cdot \mathbf{k} + i\mu\boldsymbol{\gamma} \cdot \mathbf{E}$ , the energy of the zero-momentum mode reads

$$\epsilon^{k=0} = \sqrt{m^2 + \mu^2 E^2} \sim m + \frac{\mu^2 E^2}{2m}. \quad (13)$$

The energy shift quadratic in the electric field forces an interpretation in terms of the polarizability of the particle, which is not associated with any actual structural deformation. We interpret the Pauli term in LHPs in a similar manner: it describes an effective polarizability of an electron (and hole) quasiparticle in LHPs, which on the microscopic level can be traced back to the local atomic polarizability of the perovskite lattice, which is large due the presence of  $\text{Pb}^{2+}$  ions. In other words, the spin-electric term  $\mu \boldsymbol{\tau}_1 \otimes \boldsymbol{\sigma} \cdot \mathbf{E}$  originates from a

coupling between valence and conduction bands that is mediated by the electric field even in the limit  $k = 0$  due to the lattice polarizability. The fact that the value of  $\mu$  was found to be considerable in LHPs [21] implies that quasi-electrons dressed by the high polarizability of lead ions obey the Dirac-Pauli equation.

To the best of our knowledge, LHP is the only known family of materials where the Pauli term cannot be neglected, providing a convenient testground to study intriguing theoretical concepts from high-energy physics. In this paper, we demonstrate some basic physical manifestations of Pauli coupling in the problems related to scattering off step potential and the spectrum of electronic bound states in the vicinity of defects. However, there are other scenarios where the effects of the Dirac-Pauli physics could be interesting to explore. For example, recent observations of the dynamical Schwinger effect [37] opens an opportunity to simulate analogues of relativistic strong-field effects, and to investigate (both theoretically and experimentally) the Pauli coupling in the presence of strong laser fields.

- 
- [1] T. Wehling, A. Black-Schaffer, and A. Balatsky, Dirac materials, *Advances in Physics* **63**, 1–76 (2014).
  - [2] A. H. Castro Neto, F. Guinea, N. M. R. Peres, K. S. Novoselov, and A. K. Geim, The electronic properties of graphene, *Reviews of Modern Physics* **81**, 109–162 (2009).
  - [3] M. Z. Hasan and C. L. Kane, Colloquium: Topological insulators, *Reviews of Modern Physics* **82**, 3045–3067 (2010).
  - [4] X.-L. Qi and S.-C. Zhang, Topological insulators and superconductors, *Reviews of Modern Physics* **83**, 1057–1110 (2011).
  - [5] N. P. Armitage, E. J. Mele, and A. Vishwanath, Weyl and Dirac semimetals in three-dimensional solids, *Reviews of Modern Physics* **90**, 015001 (2018).
  - [6] M. E. Peskin and D. V. Schroeder, *An Introduction to Quantum Field Theory* (Westview Press, 1995).
  - [7] L. L. Foldy, The electromagnetic properties of dirac particles, *Phys. Rev.* **87**, 688 (1952).
  - [8] W. Pauli, Relativistic field theories of elementary particles, *Reviews of Modern Physics* **13**, 203–232 (1941).
  - [9] V. G. Bagrov and D. Gitman, *The Dirac Equation and its Solutions* (De Gruyter, Berlin, Boston, 2014).
  - [10] S. Weinberg, *The Quantum Theory of Fields* (Cambridge University Press, 1996).
  - [11] Recently, it was proposed that the Pauli term can be important in the context of the Landau pole [38, 39]. This however does not change the fact that the value of  $\mu'$  must be negligibly small.
  - [12] J. L. Powell, Note on the bremsstrahlung produced by protons, *Physical Review* **75**, 32–34 (1949).
  - [13] L. L. Foldy, Electric polarizability of the neutron, *Phys. Rev. Lett.* **3**, 105 (1959).
  - [14] M. Bawin and S. A. Coon, Dirac-Foldy term and the electromagnetic polarizability of the neutron, *Physical Review C* **55**, 419–423 (1997).
  - [15] M. Grätzel, The light and shade of perovskite solar cells, *Nature Materials* **13**, 838–842 (2014).
  - [16] Y. Zhao and K. Zhu, Organic-inorganic hybrid lead halide perovskites for optoelectronic and electronic applications, *Chemical Society Reviews* **45**, 655–689 (2016).
  - [17] M. V. Kovalenko, L. Protesescu, and M. I. Bodnar-chuk, Properties and potential optoelectronic applications of lead halide perovskite nanocrystals, *Science* **358**, 745–750 (2017).
  - [18] H. Jin, J. Im, and A. J. Freeman, Topological insulator phase in halide perovskite structures, *Physical Review B* **86**, 121102 (2012).
  - [19] M. A. Becker, R. Vaxenburg, G. Nedelcu, P. C. Ser-cel, A. Shabaev, M. J. Mehl, J. G. Michopoulos, S. G. Lambrakos, N. Bernstein, J. L. Lyons, T. Stöferle, R. F. Mahrt, M. V. Kovalenko, D. J. Norris, G. Rainò, and A. L. Efros, Bright triplet excitons in caesium lead halide perovskites, *Nature* **553**, 189–193 (2018).
  - [20] A. G. Volosniev, A. S. Kumar, D. Lorenc, Y. Ashour-ishokri, A. A. Zhumeckenov, O. M. Bakr, M. Lemeshko, and Z. Alpichshev, Effective model for studying optical properties of lead halide perovskites, *Phys. Rev. B* **107**, 125201 (2023).
  - [21] A. G. Volosniev, A. Shiva Kumar, D. Lorenc, Y. Ashourishokri, A. A. Zhumeckenov, O. M. Bakr, M. Lemeshko, and Z. Alpichshev, Spin-electric coupling in lead halide perovskites, *Phys. Rev. Lett.* **130**, 106901 (2023).
  - [22] T. Umabayashi, K. Asai, T. Kondo, and A. Nakao, Electronic structures of lead iodide based low-dimensional crystals, *Phys. Rev. B* **67**, 155405 (2003).
  - [23] E. Kane, Chapter 3 (the  $k \cdot p$  method), in *Semiconductors and Semimetals*, Vol. 1, edited by R. Willardson and A. C. Beer (Elsevier, 1966) pp. 75–100.
  - [24] S. L. Chuang, *Physics of Optoelectronic Devices (First ed.)* (New York: Wiley, 1995).
  - [25] H. Zhang, C.-X. Liu, X.-L. Qi, X. Dai, Z. Fang, and S.-

- C. Zhang, Topological insulators in  $\text{Bi}_2\text{Se}_3$ ,  $\text{Bi}_2\text{Te}_3$  and  $\text{Sb}_2\text{Te}_3$  with a single Dirac cone on the surface, *Nature Physics* **5**, 438–442 (2009).
- [26] O. Klein, Die Reflexion von Elektronen an einem Potentialsprung nach der relativistischen Dynamik von Dirac, *Zeitschrift fuer Physik* **53**, 157–165 (1929).
- [27] F. Sauter, Zum “Kleinschen Paradoxon”, *Zeitschrift für Physik* **73**, 547–552 (1932).
- [28] A. Hansen and F. Ravndal, Klein’s paradox and its resolution, *Physica Scripta* **23**, 1036 (1981).
- [29] N. Dombey, Seventy years of the Klein paradox, *Physics Reports* **315**, 41–58 (1999).
- [30] A. Calogeracos and N. Dombey, History and physics of the Klein paradox, *Contemporary Physics* **40**, 313–321 (1999).
- [31] The exception is electron beams in aligned crystals, which however can only be used for indirect studies of Klein paradox [40].
- [32] M. I. Katsnelson, K. S. Novoselov, and A. K. Geim, Chiral tunnelling and the Klein paradox in graphene, *Nature Physics* **2**, 620–625 (2006).
- [33] A. F. Young and P. Kim, Quantum interference and Klein tunnelling in graphene heterojunctions, *Nature Physics* **5**, 222–226 (2009).
- [34] S. Longhi, Klein tunneling in binary photonic superlattices, *Physical Review B* **81**, 075102 (2010).
- [35] L. V. Keldysh, Deep levels in semiconductors, *Sov. Phys. JETP* **18**, 253 (1964).
- [36] J. D. Bjorken and S. D. Drell, *Relativistic quantum mechanics* (McGraw-Hill Book Company, 1964).
- [37] D. Lorenc, A. G. Volosniev, A. A. Zhumekenov, S. Lee, M. Ibáñez, O. M. Bakr, M. Lemesko, and Z. Alpichshev, Dynamical Schwinger effect in lead-halide perovskites (2024), arXiv:2406.05032 [cond-mat.mes-hall].
- [38] D. Djukanovic, J. Gegelia, and U.-G. Meißner, Triviality of quantum electrodynamics revisited, *Communications in Theoretical Physics* **69**, 263 (2018).
- [39] H. Gies and J. Ziebell, Asymptotically safe QED, *The European Physical Journal C* **80**, 607 (2020).
- [40] C. F. Nielsen, R. Holtzapple, M. M. Lund, J. H. Surrow, A. H. Sørensen, M. B. Sørensen, and U. I. Uggerhøj (CERN NA63), Precision measurement of trident production in strong electromagnetic fields, *Phys. Rev. Lett.* **130**, 071601 (2023).
- [41] M. Calkin, D. Kiang, and Y. Nogami, Proper treatment of the delta function potential in the one-dimensional Dirac equation, *American Journal of Physics* **55**, 737 (1987).

#### IV. SUPPLEMENTARY 1

*Formalism.*— In this Supplementary note, we derive Eq. (7) of the main text. To this end, we consider a one-dimensional problem with  $\mathcal{E} > \Delta/2$ :

$$\left(\frac{\Delta}{2} + V(x) - \mathcal{E}\right) \psi_{\uparrow\uparrow} + \left(\mu E_x - 2at \frac{d}{dx}\right) \psi_{\downarrow\downarrow} = 0 \quad (14)$$

$$\left(-\frac{\Delta}{2} + V(x) - \mathcal{E}\right) \psi_{\downarrow\downarrow} + \left(\mu E_x + 2at \frac{d}{dx}\right) \psi_{\uparrow\uparrow} = 0 \quad (15)$$

where  $V(x)$  is the potential energy given by  $V(x) = qV_0\Theta(x)$ . The strength of the potential is determined by  $qV_0 > 0$  and its shape is described by the Heaviside step-function  $\Theta(x) = \begin{cases} 1 & \text{if } x \geq 0 \\ 0 & \text{if } x < 0 \end{cases}$ . The associated electric field is  $E_x = -V_0\delta(x)$ , where  $\delta(x)$  is the Dirac delta function. Due to the presence of the  $\delta$ -function, the spinor components are no longer continuous at  $x = 0$ . Below, we find the corresponding discontinuity condition.

To regularize the problem for  $\mu = 0$ , one can consider the  $\delta$ -function as a limit  $\delta(x) = \lim_{w \rightarrow 0} f(x)$  where  $f(x) = \begin{cases} 0 & \text{if } |x| > w \\ \frac{1}{2w} & \text{if } |x| < w \end{cases}$  [41]. As we shall show, one can do the same for  $\mu \neq 0$ . The only complication in comparison to Ref. [41] is the existence of  $V(x)$  that should change linearly in the region  $|x| < w$  to make the limiting procedure consistent. To demonstrate that this linear change does not affect the discussion in Ref. [41], we integrate Eq. (14) from  $-w$  to  $w$

$$\left(\frac{\Delta}{2} - \mathcal{E}\right) \int_{-w}^w \psi_{\uparrow\uparrow} dx + \int_{-w}^w \psi_{\uparrow\uparrow} V(x) dx = \mu V_0 \int_{-w}^w \frac{1}{2w} \psi_{\downarrow\downarrow} dx + 2at \int_{-w}^w \frac{d\psi_{\downarrow\downarrow}}{dx} dx. \quad (16)$$

The left-hand-side of this equation vanishes in the limit  $w \rightarrow 0$ , also the potential  $V(x) \ll f(x)$  for  $|x| < w$  allowing us to approximate the wave functions  $\psi_{\downarrow\downarrow}$  and  $\psi_{\uparrow\uparrow}$  for  $|x| < w$  with those for  $V(x) = 0$ . With these observations in mind, one follows Ref. [41] to derive the boundary condition

$$\frac{\psi_{\uparrow\uparrow}(w)}{\psi_{\uparrow\uparrow}(-w)} = e^{\frac{\mu V_0}{2at}}, \quad \frac{\psi_{\downarrow\downarrow}(w)}{\psi_{\downarrow\downarrow}(-w)} = e^{-\frac{\mu V_0}{2at}}. \quad (17)$$

*Solution.* – We look for a scattering solution to Eqs. (14) and (15) in the form  $\Psi^T = (\psi_{\uparrow\uparrow}, \psi_{\downarrow\downarrow})$

$$\Psi(x < 0) = A \begin{pmatrix} 1 \\ \lambda \end{pmatrix} e^{ikx} + B \begin{pmatrix} 1 \\ -\lambda \end{pmatrix} e^{-ikx}, \quad \Psi(x > 0) = C \begin{pmatrix} 1 \\ \Lambda \end{pmatrix} e^{iKx}, \quad (18)$$

where  $k = \sqrt{\mathcal{E}^2 - \frac{\Delta^2}{4}}/(2at)$  and  $K = \sqrt{(\mathcal{E} - qV_0)^2 - \frac{\Delta^2}{4}}/(2at)$  represent the electron momenta for  $x < 0$  and  $x > 0$ , respectively;  $\lambda = i2atk/(\frac{\Delta}{2} + \mathcal{E})$  and  $\Lambda = i2atK/(\frac{\Delta}{2} + \mathcal{E} - qV_0)$ . The coefficients  $A$ ,  $B$  and  $C$  are derived from the discontinuity relation at  $x = 0$ :

$$C = (A - B)e^{-\frac{\mu V_0}{2at}} \frac{\lambda}{\Lambda}, \quad C = (A + B)e^{\frac{\mu V_0}{2at}}. \quad (19)$$

The corresponding reflection and transmission coefficients are calculated using the current densities of incoming and outgoing waves. To define them, we first write Eqs. (14) and (15) in a compact form for  $|x| \rightarrow \infty$

$$\left[\sigma_z \frac{\Delta}{2} + (V(x) - i\partial_t)\mathbb{I} - 2iat\sigma_y\partial_x\right]\Psi = 0. \quad (20)$$

Note that this equation does not have any information about the Pauli term, and hence we can use the standard definition of the Dirac current: by first multiplying Eq. (20) by  $\Psi^\dagger$  from the left and the Hermitian transpose of this equation with  $\Psi$  from the right, and then subtracting the outcomes, we derive

$$\partial_t(\Psi^\dagger\Psi) + 2at\partial_x(\Psi^\dagger\sigma_y\Psi) = 0. \quad (21)$$

This equation defines the current density as  $j = 2at(\Psi^\dagger\sigma_y\Psi)$ . The reflection and transmission coefficients can be now defined as  $R = \frac{j_{\text{reflected}}}{j_{\text{incident}}} = \left|\frac{B}{A}\right|^2$  and  $T = \frac{j_{\text{transmitted}}}{j_{\text{incident}}} = \left|\frac{C}{A}\right|^2 \frac{\text{Im}\Lambda}{\lambda}$ , respectively, leading to the result presented in the main text.

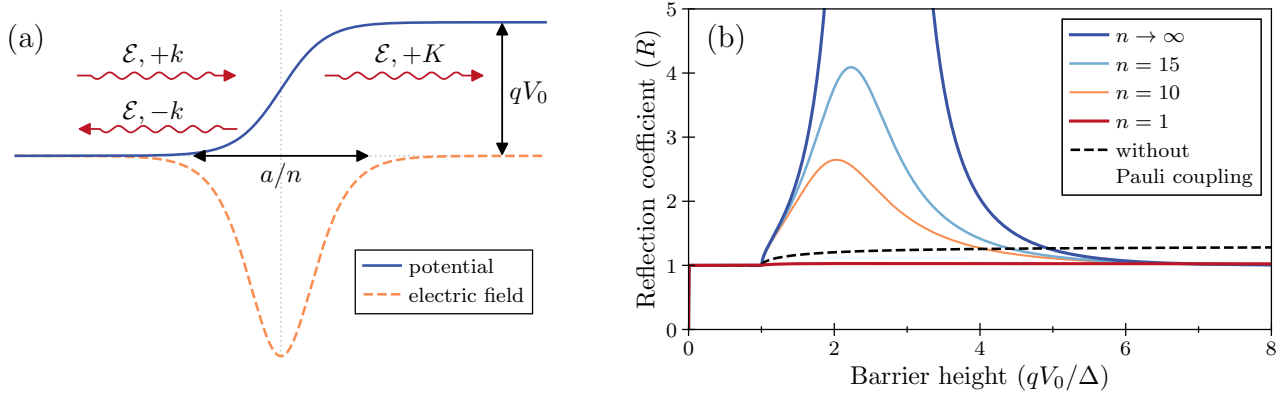


FIG. 3. (a) Sketch of a smooth potential barrier from Eq. (22). (b) The reflection coefficient as a function of the (dimensionless) barrier height for different steepness of the potential, which is characterized by  $n$ . The figure is for  $\mu > 0$ .

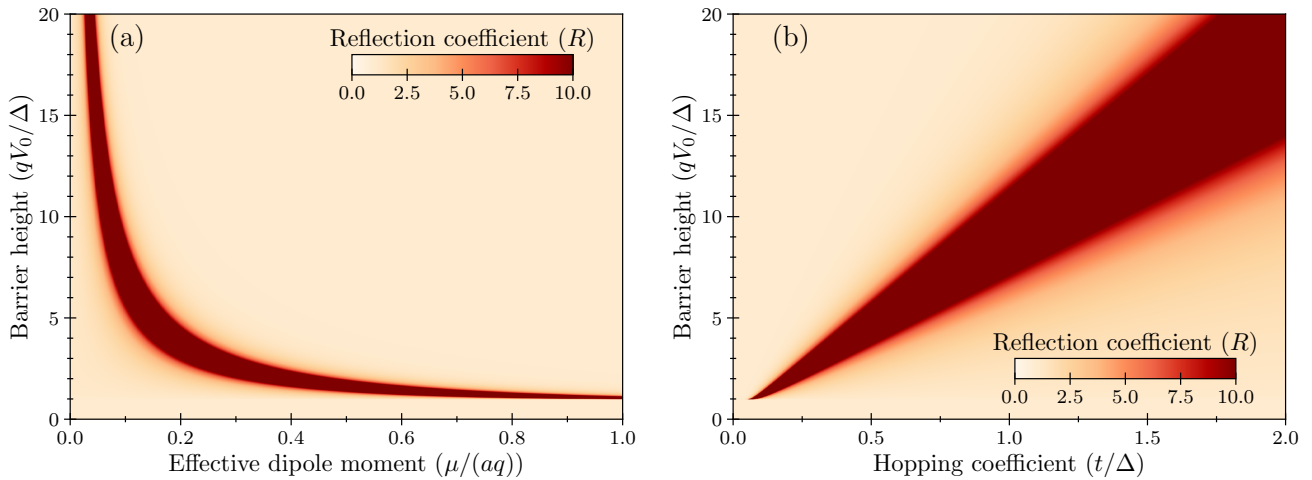


FIG. 4. Reflection coefficient ( $R$ ) as a function of the (dimensionless) barrier height  $qV_0/\Delta$  and: (a) (dimensionless) effective dipole moment  $\mu/(aq)$ ; (b) (dimensionless) hopping coefficient  $t/\Delta$ .

## V. SUPPLEMENTARY 2

Here, we consider the case of  $\mu > 0$ . In comparison to the case of  $\mu < 0$  considered in the main text, the major difference is the occurrence of a resonance at the barrier height corresponding to vanishing denominators in Eq. (7) of the main text, i.e., for  $r = -1$ , see Fig. 3(b). It can be demonstrated that this resonance is not a mathematical artefact of the employed step potential by using in Eqs. (14) and (15) a hyperbolic tangent potential

$$V(x) = \frac{qV_0}{2} \left[ \tanh\left(\frac{nx}{a}\right) + 1 \right], \quad (22)$$

standard in the studies of Klein paradox [27]. Here,  $n$  characterises the steepness of the potential, see Fig. 3(a). Figure 4 shows how the resonance is modified as a function of other parameters.

## VI. SUPPLEMENTARY 3

Here, we present technical details for bound-state calculations presented in the main text. For convenience, we write the equation  $H\Psi = \mathcal{E}\Psi$ , where  $H$  is a  $4 \times 4$  matrix and  $\Psi = \begin{pmatrix} \psi_{\uparrow} \\ \psi_{\downarrow} \end{pmatrix}$  ( $\psi_{\uparrow}$ : the electron manifold;  $\psi_{\downarrow}$ : the hole



manifold) as

$$H_{aa}\psi_{\uparrow} + H_{ab}\psi_{\downarrow} = 0 \quad (23a)$$

$$H_{ba}\psi_{\uparrow} + H_{bb}\psi_{\downarrow} = 0 \quad (23b)$$

where  $H_{aa} = H_{11} - \mathcal{E}$ ,  $H_{bb} = H_{22} - \mathcal{E}$ ,  $H_{ab} = H_{12}$ ,  $H_{ba} = H_{21}$ . Here  $H_{ij}$  is the  $ij^{\text{th}}$   $2 \times 2$  block of the Hamiltonian. Substituting  $\psi_{\downarrow}$  from Eq. (23b) into Eq. (23a) and introducing  $[H_{ab}H_{bb}]$ , it takes the form

$$(H_{ab}H_{ba} - H_{bb}H_{aa} - [H_{ab}H_{bb}]H_{bb}^{-1}H_{ba})\psi_{\uparrow} = 0. \quad (24)$$

We make this equation dimensionless by dividing it with the mass term of the Dirac equation,  $\Delta$ :

$$(H_0 + H')\psi_{\uparrow} = 0, \quad \text{where} \quad H_0 = \frac{1}{\Delta}(H_{ab}H_{ba} - H_{bb}H_{aa}) \quad \text{and} \quad H' = -\frac{1}{\Delta}[H_{ab}H_{bb}]H_{bb}^{-1}H_{ba}. \quad (25)$$

In our analysis,  $H_0$  is the leading-order Hamiltonian in the powers of  $\Delta$ ;  $H'$  is  $1/\Delta^2$ -perturbation (recall that  $H_{bb}^{-1} \sim 1/\Delta$ ).

Let us calculate the Hamiltonian  $H_0$  for a slowly changing electric field whose effect can be taken into account within the local density approximation. To this end, we derive

$$H_{ab}H_{ba} = -4a^2t^2\nabla^2 - 2at\mu\nabla \cdot \mathbf{E}(\mathbf{r}) - i2at\mu\boldsymbol{\sigma} \cdot (\nabla \times \mathbf{E}(\mathbf{r})) + i4at\mu\boldsymbol{\sigma} \cdot (\mathbf{E}(\mathbf{r}) \times \nabla) + \mu^2|\mathbf{E}(\mathbf{r})|^2, \quad (26)$$

$$-H_{bb}H_{aa} = \left(\frac{\Delta^2}{4} - \epsilon^2\right) - \frac{t_3a^2\Delta}{4}\nabla^2 + 2\epsilon q\phi(r) - (q\phi(r))^2 + \frac{t_3a^2}{4}(q\phi(r)\nabla^2 - q\nabla^2\phi(r)). \quad (27)$$

Note that  $\nabla \times \mathbf{E} = 0$  since we are dealing with a time-independent problem; further,  $\boldsymbol{\sigma} \cdot (\mathbf{E} \times \nabla) = i2\frac{|\mathbf{E}(r)|}{r}\mathbf{S} \cdot \mathbf{L}$  for a spherically symmetric problem with  $\mathbf{S} = \boldsymbol{\sigma}/2$  ( $\mathbf{L} = -i(\mathbf{r} \times \nabla)$ ) being the standard spin (angular momentum) operator. Hence, equation (26) becomes

$$H_{ab}H_{ba} = -4a^2t^2\nabla^2 - 2at\mu\nabla \cdot \mathbf{E}(\mathbf{r}) + \mu^2|\mathbf{E}(\mathbf{r})|^2 - 8at\mu\frac{|\mathbf{E}(r)|}{r}\mathbf{S} \cdot \mathbf{L}. \quad (28)$$

Furthermore, we have that  $\langle f|\nabla^2\phi(r)|f\rangle = \langle f|\phi(r)\nabla^2|f\rangle$  for any square integrable function  $f$ . Therefore, the last term in Eq. (27) can be neglected.

Introducing the notation:  $\mathcal{E} = \frac{\Delta}{2} + \epsilon$ , where  $\epsilon \ll \frac{\Delta}{2}$ , we write down the Hamiltonian  $H_0$  as

$$H_0 = -\frac{4a^2t^2}{\Delta}\nabla^2 - \frac{t_3a^2}{4}\nabla^2 + \frac{\mu^2|\mathbf{E}(\mathbf{r})|^2}{\Delta} - \frac{2at\mu}{\Delta}\nabla \cdot \mathbf{E}(\mathbf{r}) - \frac{8at\mu}{\Delta}\frac{|\mathbf{E}(r)|}{r}\mathbf{S} \cdot \mathbf{L} - \epsilon + q\phi(r) - \frac{q^2\phi(r)^2}{\Delta}, \quad (29)$$

where  $-\frac{2at\mu}{\Delta}\nabla \cdot \mathbf{E}(\mathbf{r})$  resembles the standard Darwin term and  $-\frac{8at\mu}{\Delta}\frac{|\mathbf{E}(r)|}{r}\mathbf{S} \cdot \mathbf{L}$  describes spin-orbit coupling. To write the corresponding Schrödinger equation, we define the effective mass of electrons in the material,  $\frac{1}{m_e^*} = \frac{8a^2t^2}{\Delta} + \frac{t_3a^2}{2}$ , so that

$$\left(-\frac{\nabla^2}{2m_e^*} + q\phi(r) - \frac{q^2\phi(r)^2}{\Delta} + H_P\right)\psi(r) = \epsilon\psi(r), \quad (30)$$

where

$$H_P = \frac{\mu^2}{\Delta}|\mathbf{E}(\mathbf{r})|^2 - \frac{2ta\mu}{\Delta}[\nabla \cdot \mathbf{E}(\mathbf{r})] - \frac{8at\mu}{\Delta}\frac{|\mathbf{E}(r)|}{r}\mathbf{S} \cdot \mathbf{L} \quad (31)$$

is the result of the Pauli term;  $\psi(r)$  is the electronic wavefunction. Using the values  $a = 0.586$  nm,  $t = 0.6$  eV,  $t_3 = 0.9$  eV and  $\Delta = 2.3$  eV, the effective mass of an electron is  $m_e^* = 0.13m_e$ , where  $m_e$  is the rest mass of a free electron.

In spherical polar coordinates, Eq. (30) can be re-written as

$$\left(-\frac{1}{2m_e^*}\frac{d^2}{dr^2} + q\phi(r) - \frac{q^2\phi(r)^2}{\Delta} + H_P\right)U(r) = \epsilon U(r) \quad (32)$$

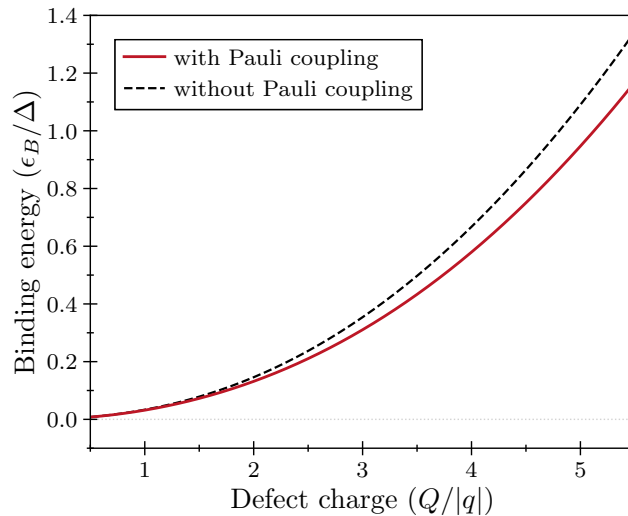


FIG. 5. Binding energy of the electron-defect bound state with (upper curve) and without (lower curve) Pauli coupling as a function of the charge of the defect.

where  $\psi(r) = \frac{1}{\sqrt{4\pi}} \frac{U(r)}{r}$ . To solve this equation numerically, we consider a finite system, i.e.,  $r \in [0, R]$ , and expand  $U(r)$  over a complete basis

$$U(r) = \sqrt{\frac{2}{R}} \sum_n \alpha_n \sin(k_n r), \quad (33)$$

where the boundary condition defines the allowed values of  $k_n$ :  $\sin(k_n R) = 0 \rightarrow k_n = \pi n/R$ ; the prefactor follows from the normalization condition  $\int_0^R dr \sin(k_i r) \sin(k_j r) = \frac{R}{2} \delta_{ij}$ . Note that we have used the fact that the three-dimensional electronic wave function must be finite at the origin for physical potentials, which implies that  $U(0) = 0$ .

Finally, we substitute Eq. (33) into Eq. (32) and obtain the linear system of equations

$$\forall j: \sum_j \left[ -\frac{k_i^2}{2m_e^*} \delta_{ij} + \frac{2}{R} \int_0^R dr \phi(r) \sin(k_i r) \sin(k_j r) + \frac{2}{R} \int_0^R dr H_P \sin(k_i r) \sin(k_j r) \right] \alpha_i = \epsilon \alpha_j. \quad (34)$$

We solve Eq. (34) numerically after introducing a momentum cutoff  $\forall i: k_i < k_{\max}$ , which leads to a finite-dimensional matrix equation that can be solved numerically using standard software. We adjust the binding energy of the electron by changing the charge of the defect,  $Q$ , see Fig. 5. Then, we produce the figure in the main text by connecting  $Q$  to the binding energy of the system without the Pauli term.